Zernike Moment-Based Subpixel Edge Detection

S. Ghosal

Department of Electrical Engineering
Center for Robotics & Mfg. Sys.
University of Kentucky
Lexington, KY 40506
Email:ghosal@ms.uky.edu

R. Mehrotra

Department of Computer Science
Center for Robotics & Mfg. Sys.
University of Kentucky
Lexington, KY 40506
Email:rajiv@ms.uky.edu

Abstract

This paper presents a new approach to detect step edges with subpixel accuracy. The proposed approach is based on a set of orthogonal complex moments of the image known as Zernike moments. An ideal 2-D step edge is modeled in terms of four parameters: the background gray level, the step size, the distance of the edge from the center of the mask, and the orientation of the edge. Discrete Zernike moments are used to obtain a total of three masks to compute all the edge parameters for subpixel detection. For pixel-level edge detection only two masks (one real and one complex) are required. The theoretical analysis of the influence of noise on the location and the orientation of an edge is presented. This analysis reveals that the accuracy of the proposed approach is virtually unaffected by the additive noise. The technique is effective in detecting both the pixel-level and subpixel-level edges. Experimental results are presented to demonstrate the efficacy of the proposed technique.

1 Introduction

In gray level images discontinuities in image intensity profiles are called edges. Detection of these discontinuities is an essential step in many machine vision tasks such as object recognition, motion analysis etc. The edge detection problem is well studied in image processing research community. But most of the efforts have focused on pixel-level edge detection. However, current trends towards digitization of analog imagery have motivated precise subpixel-level edge detection techniques. Traditionally, high precision edge detection has been accomplished by increasing sampling rate. However, maximum sampling rate is limited by physical devices. There are some applications like photogrammetry, manufacturing, remote sensing, satellite imagery etc., where desired measurement accuracy can only be attained by direct sub-pixel level operations [1].

A few techniques for subpixel step edge detection have been reported in the literature. Some of these techniques evaluate gray-level or geometric moments to determine various parameters of a sub-pixel edge, whereas others employ surface fitting or interpolation approach to detect sub-pixel edges. One of earliest reported techniques in sub-pixel edge detection is due to Hueckel [6]. He determined the edge parameters by fitting image data to a Hilbert space of nine parameters. Then the computed edge parameters are compared with an ideal edge profile. A point is declared an edge point if the computed edge parameter values at that point are sufficiently close to the ideal edge model. This operator performs poorly at isolated edge points. MacVicar-Whelan and Binford suggested detection of sub-pixel edges by linearly interpolating the location within a rise-fall-rise region of a smoothed gradient image [2]. This operator is less prone to noise compared to other gradient operators, but it has a limited precision due to interpolation. Huertas and Medioni used facet model combined with LoG masks [5] to detect sub-pixel edges. This operator detects edges from the zero-crossing in the response of LoG mask. Subpixel edge locations are obtained by using a two-dimensional second order polynomial facet model in a neighborhood of the filtered image. Among the moment-based techniques, Machuca and Gilbert proposed a method which integrates the region containing the edge [3]. This method uses the moments found in the region to determine the edge location. In this method, the "center of mass" around the neighborhood of a point is calculated by using different geometric moments and for an edge point the distance of the "center of mass" from the point should have a high value. This method is computationally less expensive compared to Hueckel's operators and can be used to detect step, ramp and roof edges. Tabatabai and Mitchell determined edge location by fitting first three gray level moments to the edge data. They have also shown that edge location is related to the so-called "Christoffel Numbers" [4]. The sub-pixel edge parameters are found as functions of gray level moments. Recently, Lyvers and Mitchell et al. proposed an efficient geometric moment-based method for subpixel edge detection [1]. This method uses six masks to evaluate different geometric moments which, in turn, are used to determine four parameters of a step edge, i.e. step height, background gray level, distance of the edge from center of the pixel and angle of the edge. These moments are basically projections of the image function onto the monomials $x^p y^q$. Unfortunately,

the basis set $\{x^p y^q\}$ is not orthogonal. Consequently, these moment-masks lack the optimality in information redundancy and other useful properties that may result from using orthogonal basis functions. Moreover, the relationships between these moments of an image and its rotated version are not simple. As a result the theoretical noise calculation becomes very complex.

In this paper, we propose orthogonal moment-based complex operators to detect step edges in an image. In fact, discrete Zernike moments of an image are used to detect edges [7]. One interesting property of Zernike moments is that their values for an image and its rotated version have simple relationships. We propose a Zernike moment-based approach to 2-D step edge detection. The proposed approach employs two masks, one real and one complex, for pixel-level edge detection and three masks, two real and one complex, for sub-pixel edge detection.

The remainder of this paper is organized as follows. Section 2 presents some background information of Zernike moments. In Section 3 we present the theory of Zernike moment-based edge detection. A theoretical noise performance model for this edge detection method is also discussed. Implementation details and some experimental results are discussed in Section 4. Finally we present our conclusions in Section 5 and mention some future research activities.

2 Zernike Moments

It can be shown that there exists an infinite complete sets of polynomials in two real variables which are orthogonal in the interior of the unit circle [10]. The circular polynomials of Zernike are distinguished from other sets by certain simple invariance properties which can be best explained from group theoretic considerations. These moments are basically projections of the image data onto a set of complex polynomials, which form a complete orthogonal set over the interior of a unit circle, i.e. $x^2 + y^2 \leq 1$. Zernike moment of order n and repetition m for an image $f(x, y)$, is defined as

$$A_{nm} = \frac{n+1}{\pi} \int\int_{x^2+y^2 \leq 1} f(x,y) V^*_{nm}(\rho, \theta) dx dy \quad (1)$$

The term outside the integral is merely a normalization factor and it is ignored in future discussion. In discrete form, A_{nm} can be expressed as

$$A_{nm} = \sum_x \sum_y f(x,y) V^*_{nm}(\rho, \theta) \quad x^2 + y^2 \leq 1 \quad (2)$$

Thus, in a discrete image, for evaluating Zernike moment A_{nm} at an image point, the neighborhood of that point should be mapped onto the interior of the unit circle. The complex polynomials V_{nm} can be expressed in polar coordinates (ρ, θ) as

$$V_{nm}(\rho, \theta) = R_{nm}(\rho) e^{jm\theta} \quad (3)$$

where $n \geq 0$, and $n - |m|$ is even positive integer. $R_{nm}(\rho)$ is a radial polynomial defined as

$$R_{nm}(\rho) = \sum_{s=0}^{(n-|m|)/2} \frac{(-1)^s (n-s)! \rho^{n-2s}}{s!(\frac{n+|m|}{2} - s)!(\frac{n-|m|}{2} - s)!} \quad (4)$$

V_{nm}s are orthogonal and satisfy the following relationship iff $n = p$ and $m = q$

$$\int\int_{x^2+y^2 \leq 1} V^*_{nm}(x,y) V_{pq}(x,y) dx dy = \frac{\pi}{n+1} \quad (5)$$

Otherwise, the integral is zero. If f(x,y) is constant inside the unit circle, this relationship is valid for A_{nm} also. An important property of Zernike moments is that their values in an image and its rotated version have simple relationship. If an image is rotated by an angle ϕ, the Zernike moments of the original image A_{uv} and the Zernike moments of the rotate image A'_{uv} are related as

$$A'_{uv} = A_{uv} e^{-jv\phi} \quad (6)$$

It is clear that Zernike moments merely acquire a phase shift on rotation and their magnitudes remain constant. This property is useful for rotation invariant pattern recognition and matching [8].

3 Zernike Moments-Based Edge Detection

Zernike moments are basically integral based operators and therefore are good candidates for noise tolerant image processing. These moments are dependent on the image data and we claim that any features resulting from image intensity profile can be described by proper Zernike moments. Here we concentrate on their use for sub-pixel and pixel-level edge detection. Consider an ideal step edge, shown in Figure 1. k is the step height, h is the background gray level, l is the perpendicular distance from the center of the circular kernel and the edge makes an angle of ϕ with respect to x-axis. If we rotate the edge by an angle $-\phi$, it will be aligned parallel to the y-axis. So, we have

$$\int\int_{x^2+y^2 \leq 1} f'(x,y) y dy dx = 0 \quad (7)$$

where $f'(x, y)$ is the edge function after it is rotated. Now, the orthogonal complex polynomials $V_{00}, V_{11}, and V_{20}$s can be written as

$$V_{00} = 1 \quad V_{11} = x - jy \quad V_{20} = 2x^2 + 2y^2 - 1$$

The corresponding Zernike moments A_{nm}s of the original image data $f(x, y)$ and A'_{nm}s of the rotated image are related by

$$A'_{00} = A_{00} \quad A'_{11} = A_{11} e^{j\phi} \quad A'_{20} = A_{20}$$

Since the expression in the in Equation (7) is the imaginary component of A'_{11}, we can write

$$Im[A'_{11}] = \sin(\phi) Re[A_{11}] + \cos(\phi) Im[A_{11}] = 0 \quad (8)$$

where $Im[A'_{11}]$ and $Re[A'_{11}]$ are the imaginary and real components of A'_{11}, respectively. Therefore,

$$\phi = tan^{-1}(\frac{Im[A_{11}]}{Re[A_{11}]}) \quad (9)$$

Referring to Figure 1, we can further calculate,

$$\begin{aligned} A'_{00} &= 2\int_{-1}^{1}\int_{0}^{\sqrt{1-x^2}} h dy dx + 2\int_{l}^{1}\int_{0}^{\sqrt{1-x^2}} k dy dx \\ &= h\pi + \frac{k\pi}{2} - k sin^{-1}(l) - kl\sqrt{1-l^2} \\ A'_{11} &= \int\int_{x^2+y^2\leq 1} f'(x,y)(x-jy)dydx \\ &= \frac{2k(1-l^2)^{3/2}}{3} \\ A'_{20} &= \int\int_{x^2+y^2\leq 1} f'(x,y)(2x^2+2y^2-1)dydx \\ &= \frac{2kl(1-l^2)^{3/2}}{3} \end{aligned}$$

Solving these equations and substituting $A'_{00} = A_{00}$ and $A'_{20} = A_{20}$, we get the other three step edge parameters:

$$l = \frac{A_{20}}{A'_{11}} \quad (10)$$

$$k = \frac{3A'_{11}}{2(1-l^2)^{3/2}} \quad (11)$$

$$h = \frac{A_{00} - \frac{k\pi}{2} + k sin^{-1}(l) + kl\sqrt{(1-l^2)}}{\pi} \quad (12)$$

Thus three Zernike moments A_{00}, A_{20}, and A_{11} are needed to calculate the four parameters of the step edge. To estimate these moments, the corresponding masks of any desired size can be obtained by evaluating the associated integral over each pixel assuming $f(x,y)$ to be constant over that pixel. Circular limits are taken for integration. The moments are estimated by correlating the image elements with the masks. Zernike moment-based edge detector employs fewer masks compared to the geometric moment-based detector. The geometric moment-based edge detector require a total of six masks [1] whereas the Zernike moment-based detector uses 3 masks. Therefore, the proposed Zernike moment-based edge detector is more efficient compared to the geometric moment-based detector.

3.1 Zernike Moments-Based Pixel-level Edge Detector

In this subsection, we develop a Zernike moment-based method for pixel-level edge detection as a special case of subpixel-level edge detection. In pixel-level edges, the distance of the edge l from the center of the mask can be taken as zero and if the detected step size k is greater than a predetermined threshold then the given pixel is marked as an edge pixel. Now, if the distance l of the edge from the center of the mask is zero, Equations (10) and (11) can be written as,

$$k = \frac{3A'_{11}}{2} \quad (13)$$

$$h = \frac{A_{00} - 0.5k\pi}{\pi} \quad (14)$$

Using Equations (9), (13) and (14), pixel-level edge parameters, i.e. the direction of the edge, step size k, and background gray level h can be calculated. Thus, one complex mask for A_{11} and one real mask for A_{00} are required to specify the three parameters of a pixel-level edge.

3.2 Stochastic Analysis

In this subsection, the influence of noise on the performance of the proposed subpixel edge detector is presented. We separately consider the effect of noise on edge location l and orientation ϕ. Assume i.i.d. Gaussian noise $\eta(x,y)$ with zero-mean and variance σ^2 is added to the pixel gray levels of a sampled ideal edge. Now, referring to Equation (10), we can write the detected random distance $\hat{l}$ of the edge as,

$$\hat{l} = \frac{A'_{20}}{A'_{11}} \quad (15)$$

where

$$A'_{20} = \sum_{i=0}^{w}\sum_{j=0}^{w} V_{20}(i,j)\hat{f}(i,j),$$

$$A'_{11} = \sum_{i=0}^{w}\sum_{j=0}^{w}(Re[V_{11}(i,j)]\hat{f}(i,j)cos(\phi) + Im[V_{11}(i,j)]\hat{f}(i,j)sin(\phi)),$$

and $\hat{f}(i,j) = f(i,j) + \eta(i,j)$ is the noisy image data and $w \times w$ is the dimension of the mask. This response can be viewed as a deterministic part plus a random part η_{nm}. Response of A_{nm} to the noise can be written as

$$\eta_{nm} = \sum_{i=0}^{w}\sum_{j=0}^{w} V^*_{nm}\eta(i,j) \quad (16)$$

Hence η_{nm} is simply the weighted sum of w x w independent, zero-mean Gaussian random variables. In presence of noise, $\hat{l}$ can be written as

$$\hat{l} = \frac{\hat{g}_n}{\hat{g}_d}$$

$$E\{\hat{g}_n\} = \mu_n = \sum_{i=0}^{w}\sum_{j=0}^{w} V_{20}(i,j)f(i,j)$$

$$E\{\hat{g}_d\} = \mu_d = \sum_{i=0}^{w}\sum_{j=0}^{w}(Re[V_{11}(i,j)]f(i,j)cos(\phi)$$

$$+Im[V_{11}(i,j)]sin(\phi))$$

standard deviation of $(\hat{g}_n)$ can be written as,

$$\sigma_n^2 = \sigma^2 \sum_{i=0}^{w}\sum_{i=0}^{w} V_{20}^2(i,j)$$

and standard deviation of $[\hat{g}_d]$ as,

$$\sigma_d^2 = \sigma^2 \sum_{i=0}^{w}\sum_{i=0}^{w}((Re[V_{11}(i,j)]])^2 cos^2(\phi) + (Im[V_{11}(i,j)]])^2 sin^2(\phi)$$

The random variable $\hat{l}$ can now be viewed as the quotient of two non-zero mean Gaussian random variables. To completely parameterize this relationship, the covariance between the numerator and denominator random variables must be determined. Now since Zernike moments are orthogonal,

$$\sum\sum V_{nm}(i,j)V_{pq}^*(i,j) = 0 \quad n \neq p \text{ or } m \neq q \quad (17)$$

After some algebraic manipulation, it is easy to show that covariance $E\{\hat{g}_n \hat{g}_d\}$ is zero. Now, if the two Gaussian variables are uncorrelated, then they are necessarily independent. Hence, the distance equation is the quotient of two non-zero independent Gaussian random variables. So we can write

$$p(\hat{g}_n, \hat{g}_d) = p_{\hat{g}_n}(g_n)p_{\hat{g}_d}(g_d) \quad (18)$$

$$p_{\hat{l}}(l) = \int_{-\infty}^{\infty} |g_d| p_{\hat{g}_n}(lg_d)p_{\hat{g}_d}(g_d)dg_d \quad (19)$$

Simplifying the above equation, we get

$$p_{\hat{l}}(l) = \int_{-\infty}^{\infty} \frac{|y|}{2\pi\sigma_n\sigma_d} e^{-(\frac{(ly-\mu_n)^2}{2\sigma_n^2} + \frac{(y-\mu_d)^2}{2\sigma_d^2})} dy \quad (20)$$

$p_{\hat{l}}(l)$ is the probability density function(PDF) of the distance of the edge. For 5 x 5 window size note, $\sigma_n^2 = 0.112\sigma^2$ and $\sigma_d^2 = 0.178\sigma^2$. After some mathematical manipulation the PDF for the distance of the edge can be written as,

$$p_{\hat{l}}(l) = \frac{\sigma_n\sigma_d}{\pi(l^2\sigma_d^2 + \sigma_n^2)} e^{-(\frac{\mu_n^2}{2\sigma_n^2} + \frac{\mu_d^2}{2\sigma_d^2})} + \sqrt{\frac{2}{\pi}} \frac{l\mu_n\sigma_d^2 + \mu_d\sigma_n^2}{(l^2\sigma_d^2 + \sigma_n^2)^{1.5}} e^{\frac{(\mu_n - l\mu_d)^2}{2(l\sigma_d^2 + \sigma_n^2)}} \gamma \quad (21)$$

where

$$\gamma = erf[\frac{\mu_d\sigma_n^2 + l\mu_n\sigma_d^2}{\sigma_n\sigma_d\sqrt{\sigma_n^2 + l^2\sigma_d^2}}]$$

It is interesting to note that the PDF of the distance of the 2-D step edge for Zernike moment-based detectors is similar in form to the PDF of the distance of a 1-D step edge for the geometric moment-based edge operators proposed in [1]. However, in our case, μ_n and μ_d are functions of the edge orientation. If the edge is oriented vertically and $\mu_n = \mu_d = 0$, the above probability density reduces to a Cauchy density.

Figure 2 shows the density functions for edges located at the center of the window and at -0.4 and +0.4 pixels from the center of the window where a 5 x 5 window is taken. The background gray level is 100 and step is also 100. The signal to noise ratio(SNR) is 30dB. Note that the peak of the density functions are slightly shifted from the actual sub-pixel edge locations. This is due to the deterministic error and the digitization of the continuous mask. The plot of theoretical density function of distance of the edge shows that the detector is quite immune to noise.

The evaluation of density function of the orientation of the 2-D step edge is quite straight forward. Zernike moments masks Re$[A_{11}]$ and Im$[A_{11}]$ are used to calculate the angle of the edge. The angle ϕ is determined by $tan^{-1}(\frac{Im[A_{11}]}{Re[A_{11}]})$. As before, $Im[A_{11}]$ and $Re[A_{11}]$ are random with Gaussian distribution when Gaussian noise $\eta(x,y)$ is added to the sampled edge image. Moreover, $Re[A_{11}]$ and $Im[A_{11}]$ are independent of each other. Thus the angle is simply a quotient of two independent Gaussian random variables with the added transformation of tan^{-1}. Then the PDF can be written as,

$$p_{\hat{\phi}}(\phi) = e^{-\frac{\mu^2}{2\sigma^2}}\{\frac{1}{2\pi} + \frac{\mu\cos(\phi-\psi)}{\sqrt{2\pi}\sigma} e^{\frac{\mu^2\cos^2(\phi-\psi)}{2\sigma^2}} \beta\} \quad (22)$$

where

$$\beta = [\frac{1}{2} + erf(\frac{\mu\cos(\phi-\psi)}{\sigma})]$$

This density function $p_{\hat{\phi}}(\phi)$ is symmetrical about $\psi = tan^{-1}(\mu_y/\mu_x)$ such that the mean value of $\hat{\phi}$ is $tan^{-1}(\mu_y/\mu_x)$. μ_y is the mean of numerator in equation (9) and μ_x is the mean of the denominator. σ^2 is the variance of both numerator and denominator and $\mu^2 = \mu_x^2 + \mu_y^2$.

Note that geometric moments can be expressed as special cases of Zernike moments and $Re[A_{11}]$ and $Im[A_{11}]$ are basically equal to the geometric moments M_{10} and M_{01}, respectively. So, the PDF of the edge orientation for the Zernike moment-based detectors is same as that for the geometric moment-based operators [1].

4 Implementations

Numerous experiments have been conducted to test the efficacy of the proposed edge detection method with various gray level images. Some of these experimental results are discussed in this section.

The main steps for pixel-level and subpixel edge detection are outlined below.

4.1 Pixel-level edge detection

- Calculate desired size masks using circular limits of integration.
- Convolve these masks with the image points to get Zernike moments A_{00}, A_{11} and A_{20}.
- Evaluate ϕ using $Re[A_{11}]$ and $Im[A_{11}]$ masks in Equation (9). This gives the direction of the edge at a particular image point.
- Calculate $A'_{11} = Re[A'_{11}] = Re[A_{11}]cos(\phi) + Im[A_{11}]sin(\phi)$. Use this value of A_{11} in equation (13) to determine the step size k.
- Evaluate background gray level h using Equation (14). The above steps are repeated for every point in the image plane to get step edge parameters at every point in the image. Now postprocessing with proper threshold selection and edge thining can be done to get the final edge image. However, postprocessing is not the main topic of this paper.

4.2 Sub-pixel edge detection

- Calculate masks of desired size using circular limits of integration.
- Convolve these masks with the image points to get Zernike moments A_{00}, A_{11} and A_{20}.
- Evaluate ϕ using $Re[A_{11}]$ and $Im[A_{11}]$ masks in Equation (9). This gives the direction of the edge at a particular image point.
- Calculate $A'_{20} = A_{20}$.
- Calculate $A'_{11} = Re[A'_{11}] = Re[A_{11}]cos(\phi) + Im[A_{11}]sin(\phi)$. Use this value of A_{11} and A'_{20} in Equation (10) to find out the distance of the edge, l from the center of the mask.
- Use Equation (11) to determine the step size, k.
- Evaluate background gray level h using Equation (12).
  These steps basically specify all sub-pixel edge parameters.

The proposed approach is implemented in C language and tested on Sequent Balance 3000 running under UNIX operating systems. In our experiments, several binary and gray level(8 bit intensity) images (both synthetic and real) have been used to test the performance of the proposed pixel and subpixel-level edge detectors. Some of these results, which are obtained using masks of size 5 × 5, are presented here. Figure 3a is a 256 × 256 image of a girl. The step height detected at every point of the image, using the pixel-level detector, is shown in Figure 3b. The darkest intensity represents the step edge with largest step size. The edge map obtained by thresholding and thinning the image in Figure 3b is shown in Figure 3c.

The proposed edge detection method assumes ideal step edge model and hence its response deteriorates at locations where roof, ramp, or other non-step edges are present. However, Zernike moment-based operators can be designed for ramp, roof, or generalized step edges (combinations of step and ramp or step and roof edges) also [9].

Figure 4 is a synthetic binary image with background gray level 90 and step size of 60. The left sided edge of the rectangle makes an angle of 272 degrees with the horizontal(or j) axis (i.e., 2 degrees with the vertical axis or i-axis). Thus, $\phi = 182$ degrees in this case. Subpixel step size, angle and distance computed using the proposed subpixel edge detector are tabulated in Table 1.

5 Conclusions

In this paper an orthogonal complex moment-based technique for subpixel and pixel-level step edge detection is proposed. A total of three masks (one complex and two real) are required to compute all the parameters of a step edge with subpixel accuracy. Pixel-level edges can be detected using only two masks (one real and one complex). A theoretical measure for delocalization in presence of additive noise is obtained in terms of actual distance and orientation of the step edge. Zernike moments are functions of shape and size of objects in an image and hence any features resulting from image intensity profile can be detected by proper Zernike moments. We have also developed a Zernike moment-based corner detection method [9]. We are currently investigating the use of Zernike moments for range image segmentation and the detection of spatiotemporal features.

Acknowledgments : This work has been partially supported by the NASA-Langley Research Center under grant no. NAG-1-1276, by Biomedical Research Support Grant Program, Division of Resources, NIH under grant no. BRSG S07 RR07114-21, and the Center of Robotics and Manufacturing Systems at the University of Kentucky.

References

[1] E.P. Lyvers, O.R. Mitchell, M.L. Akey and A.P. Reeves, , *Subpixel measurements using a moment-based edge operator,* IEEE Trans. on PAMI, vol. 11 no. 12, pp. 1293-1308 (1989).

[2] P.J. MacVicar-Whelan and T.O. Binford, *Line finding with subpixel precision,* in Proc. SPIE, vol. 281, pp. (1981).

[3] R. Machuca and A.L. Gilbert, *Finding edges in noisy scenes,* IEEE Trans. on PAMI, vol. 3, no. 1, pp. 103-111, (1981).

[4] A.J. Tabatabai and O.R. Mitchell, *Edge location to subpixel values in digital imagery,* IEEE Trans. on PAMI, vol. 6, no. 2, pp. 188-201, (1984).

[5] A. Huertas and G. Medioni, *Detection of intensity changes with subpixel accuracy using Laplacian-Gaussian masks,* IEEE Trans. on PAMI, vol. 8, no. 5, pp. 651-664, (1986).

[6] M.H. Hueckel, *An operator which locates edges in digitized pictures* in J. ACM, vol. 18, pp. 113-125, (1971).

[7] F. Zernike, *Physica,* vol. 1, pp. 689, (1934).

[8] A. Khotanzad and J. Lu, *Classification of invariant image representations using a neural network,* IEEE Trans. on Acoustics, Speech and Signal Processing, vol. 38, no. 6, pp. 1028-1038 (1990).

[9] S. Ghosal and Rajiv Mehrotra, *Orthogonal moment operators for feature detection,* Technical Report, Center of Robotics and Manufacturing Systems, University of Kentucky (1991).

[10] M. Born and E. Wolf, *Principles of Optics,* Peragamon, Pergamon, pp. 767-772, (1975).

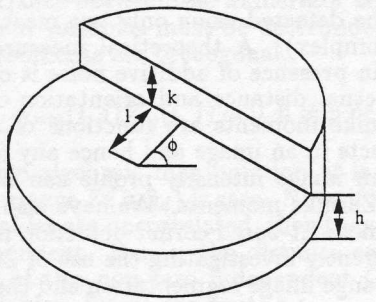

Figure 1: Two dimensional edge model

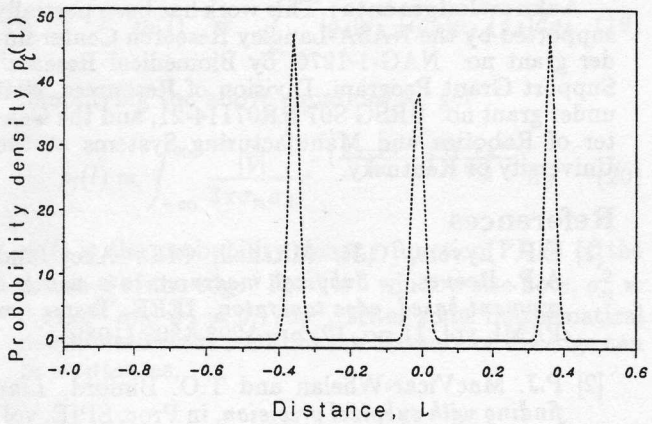

Figure 2: Theoretical probability density function

i	j	Angle, φ	Distance, l	Step Size, k
102	100	182.0058	0.1858	59.532
103	100	182.0058	0.1719	59.073
104	100	182.0058	0.1580	58.656
105	100	182.0058	0.1440	58.278
106	100	182.0058	0.1301	57.938
107	100	182.0058	0.1161	57.636
108	100	182.0058	0.1022	57.370

Table 1: Subpixel edge parameters for the image in Fig. 4

Figure 3a: Input Image

Figure 3b: Detected step heights

Figure 3c: Thinned Edge map

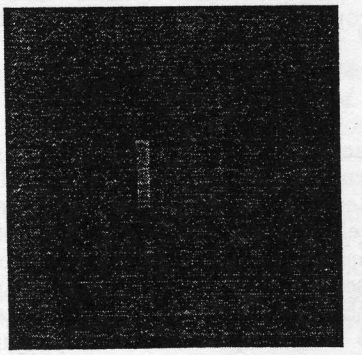

Figure 4: Binary image with subpixel edges